Supraglacial forcing of subglacial drainage in the ablation zone of the Greenland ice sheet

Ian Bartholomew,[1] Peter Nienow,[1] Andrew Sole,[1] Douglas Mair,[2] Thomas Cowton,[1] Steven Palmer,[3] and Jemma Wadham[4]

Received 8 February 2011; revised 5 March 2011; accepted 16 March 2011; published 21 April 2011.

[1] We measure hydrological parameters in meltwater draining from an outlet glacier in west Greenland to investigate seasonal changes in the structure and behaviour of the hydrological system of a large catchment in the Greenland ice sheet (GrIS). Our data reveal seasonal upglacier expansion and increase in hydraulic efficiency of the subglacial drainage system, across a catchment >600 km^2, to distances >50 km from the ice-sheet margin. This expansion occurs episodically in response to the drainage of surface meltwaters into a hitherto inefficient subglacial drainage system as new input locations become active progressively further upglacier; this system is similar to Alpine glaciers. These observations provide the first synopsis of seasonal hydrological behaviour in the ablation zone of the GrIS. **Citation:** Bartholomew, I., P. Nienow, A. Sole, D. Mair, T. Cowton, S. Palmer, and J. Wadham (2011), Supraglacial forcing of subglacial drainage in the ablation zone of the Greenland ice sheet, *Geophys. Res. Lett.*, *38*, L08502, doi:10.1029/2011GL047063.

1. Introduction

[2] In land-terminating sections of the GrIS, meltwater production enhances ice motion through seasonal velocity variations that are initiated when surface meltwaters gain access to the ice-bed interface [*Zwally et al.*, 2002]. A positive feedback between surface melting and ice velocities would accelerate mass loss from the GrIS in a warmer climate [*Zwally et al.*, 2002; *Parizek and Alley*, 2004; *Shepherd et al.*, 2009]. On the basis of correlations between ice motion and surface melting, however, it has been shown that a key control on the relationship between surface melting and ice velocity variations is the structure and hydraulic efficiency of the subglacial drainage system, which develops spatially and temporally on a seasonal basis [*Bartholomew et al.*, 2010]. A more efficient subglacial drainage system can conduct large discharges in discrete channels which operate at a lower steady-state water pressure, thereby reducing the basal lubrication effect of external meltwater inputs [*Kamb*, 1987; *Pimentel and Flowers*, 2011; *Schoof*, 2010; *Sundal et al.*, 2011].

[3] Despite the clear link between rates of ice motion and the structure of the subglacial drainage system, predictions about the future extent and magnitude of hydrologically-forced ice velocity changes in the GrIS remain uncertain [*Van de Wal et al.*, 2008]. To address this, we need to understand how spatial and temporal changes in surface melting of the GrIS force development of an efficient subglacial drainage system on a seasonal basis [*Pimentel and Flowers*, 2011; *Schoof*, 2010]. Here we present observations from Leverett Glacier, a land-terminating outlet glacier at ~67°N in west Greenland (Figure 1) in 2009, that elucidate seasonal development of the drainage system of a large catchment in the ablation zone of the GrIS.

2. Data and Methods

[4] Drainage from Leverett Glacier occurs through one large portal on the North side of the glacier snout, which grows in size over the melt season and is the outlet for runoff from a large subglacial conduit. Water stage, electrical conductivity (EC) and turbidity were monitored continuously in the proglacial stream at a stable bedrock section ~2 km downstream from the glacier terminus from May 18th 2009, before melting had started, until September 3rd. Stage was converted into discharge (Q) using a rating curve ($r = 0.92$) derived from 29 repeat dye-dilution gauging tests conducted in the proglacial stream across the full range of discharges. Uncertainty in the discharge record is the result of measurement error and application of a rating curve, and is estimated to be ±15%. A relationship between turbidity and suspended sediment concentration (SSC) was derived by calibration against 49 manual gulp sediment samples ($r = 0.91$). Uncertainties in the SSC and EC record are estimated to be ±7% and ±10% respectively. Our monitoring station was located in a single channel close to the ice margin that did not overflow at peak discharge. During a 2 week period simultaneous measurements of SSC and EC were taken within 50 m of the glacier snout, showing that the hydrological parameters we measured did not change significantly following emergence of the meltwaters from the glacier terminus.

[5] A surface digital elevation model [*Palmer et al.*, 2011] was used to derive a first approximation of the Leverett Glacier hydrological catchment (Figure 1). Although there is uncertainty in this approach, lack of appropriate bed elevation data prevents an estimate of catchment geometry based on calculations of subglacial hydraulic potential [*Shreve*, 1972]. We used satellite observations from the Moderate-resolution Imaging Spectrometer (MODIS) to study the development and drainage of supraglacial lakes within the Leverett catchment [*Sundal et al.*, 2009; *Box and Ski*, 2007]. 40 MODIS images were used spanning the period 31st May to 18th August, representing all days when lake identification was not impeded by cloud cover.

[1]School of Geosciences, University of Edinburgh, Edinburgh, UK.
[2]School of Geosciences, University of Aberdeen, Aberdeen, UK.
[3]School of Earth and Environment, University of Leeds, Leeds, UK.
[4]School of Geographical Sciences, University of Bristol, Bristol, UK.

0094-8276/11/2011GL047063

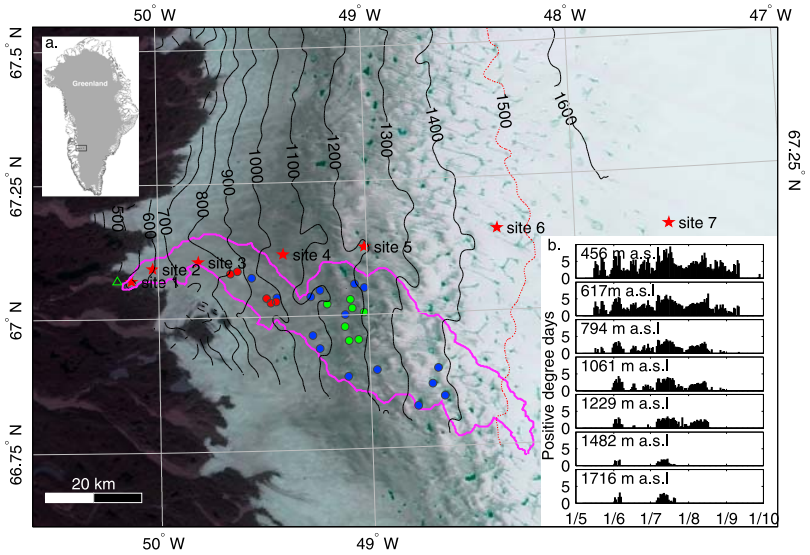

Figure 1. (a) Map showing the location of Leverett Glacier, a catchment derived from the surface DEM (purple), and locations of temperature measurements (red stars). Lakes that drain during the survey period are denoted by circles, colour-coded to show drainage events that coincide with meltwater pulses P2 (red) and P4 (green). Lakes which drain during the survey period but are not clearly associated with pulses in the discharge record are coloured blue. The location of the bedrock section where stage, EC and turbidity were measured is shown by the green triangle. (b) Positive degree-days at each of the temperature measurement locations (sites 1–7).

There is significant uncertainty in applying a depth-retrieval algorithm based on surface reflectance to find the depth of GrIS supraglacial lakes shallower than 2.5 m [*Box and Ski*, 2007]. Therefore, we used a modelled estimate [*McMillan et al.*, 2007] of the average depth of supraglacial lakes obtained within this region to estimate volumes of lakes that drain from the ice sheet surface. Continuous measurements of air temperature were made at seven sites, from 450–1700 m altitude (Figure 1). Ablation rates were also monitored using measurements of surface lowering from ultrasonic depth gauges in order to constrain a temperature-melt index model which we used to predict volumes of runoff generated from the catchment during our survey period.

3. Hydrological Observations

[6] The proglacial runoff hydrograph (Figure 2a) shows that, prior to June 1st, discharge was <6 m^3 s^{-1} during a period of ~20 days of above-zero temperatures extending up to 1400 m altitude (Figure 2d). Discharge then increased rapidly over 3 days to 46 m^3 s^{-1} on June 4th and continued to grow episodically before rising dramatically, by 220 m^3 s^{-1} in 10 days, to a peak of 317 m^3 s^{-1} on July 16th. Following this peak, discharge declined gradually but remained 3–4 times greater than early-season levels until late August. Proglacial runoff showed clear diurnal cycles which had greatest amplitude (~25 m^3 s^{-1}) later in the season, after July 16th, and were more subdued (~6 m^3 s^{-1}) earlier in the summer.

[7] The rising limb of the seasonal hydrograph is also marked by four distinct pulses of water, superimposed on the general pattern of runoff growth. These pulses each last a few days, and contribute between 4.9–11.8 × 10^6 m^3 of water to the total runoff. These pulses are also defined by coincident spikes in the EC and SSC records (Figures 2a–2c). The first pulse of water (P1 on June 3rd) marks the start of significant runoff growth. It was followed by further pulses (P2–P4) starting on June 7th, June 17th and July 3rd (Figure 2a).

[8] Maximum EC (69.9 μS cm^{-1}) occurred while discharge was still low at the beginning of the season and declined in a stepwise fashion to a minimum of 9.9 μS cm^{-1} on July 3rd, immediately prior to P4 (Figure 2b). There is a negative relationship between EC and discharge over the whole melt season (R^2 = 0.27). Following P4 EC remains low (<20 μS cm^{-1}) and the daily cycles of Q and EC develop a characteristic inverse relationship [*Fenn*, 1987] with clear stable hysteresis where EC is highest on the rising limb of the diurnal hydrograph (auxiliary material).[1] However, the relationship is not consistent throughout the survey period (Figure 2e), and early in the season can fluctuate between strong positive and strong negative relationships over short time-scales (<1 week). In particular, P1, P2 and P4 are characterized by pronounced conductivity peaks (Figure 2b) that show a strong positive relationship with increasing Q on their rising limbs (Figure 2e). During P2, EC increases from 17–42 μS cm^{-1} in 9 hours as Q increases from 40–59 m^3 s^{-1} and, during P4, EC increases from 10–40 μS cm^{-1} in 6 hours as Q increases from 74–140 m^3 s^{-1}. In these pulses, an EC peak shortly precedes maximum discharge, and EC returns to pre-pulse levels within a few days (Figure 2b). By contrast, there is no large peak in EC associated with P3.

[9] Suspended sediment concentration ranged from less than 0.2 kg m^{-3} to greater than 18 kg m^{-3}, beyond the range of our sensor, and increased gradually but episodically throughout the season (Figure 2c). In common with the pattern in electrical conductivity and discharge, there are

[1] Auxiliary materials are available in the HTML. doi:10.1029/2011GL047063.

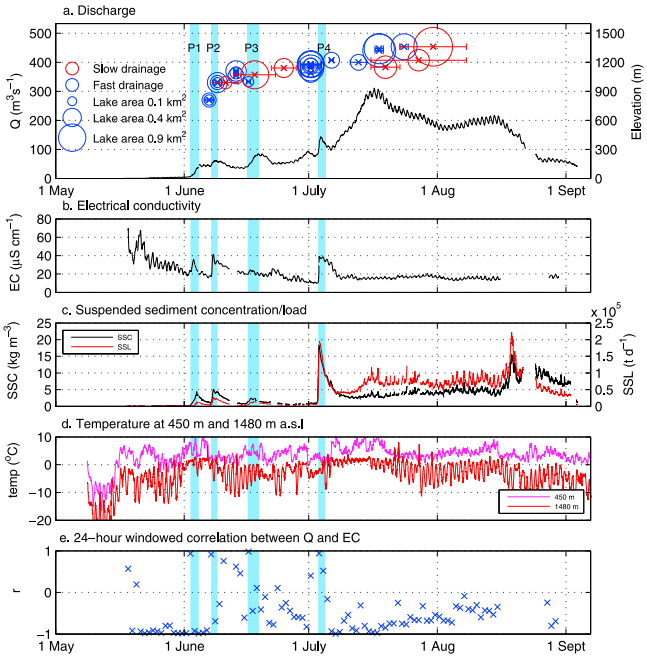

Figure 2. (a) Proglacial meltwater stream discharge ($m^3\ s^{-1}$; black line; shaded blue sections show the pulses of meltwater (P1–P4) which are superimposed on the rising limb of the seasonal runoff hydrograph). Timing, area and elevation of lake drainage events. Each circle represents a single lake drainage event, based on change in surface area on MODIS images. Horizontal bars represent the time period in which drainage took place. Red circles are lakes that drained slowly over several images while blue circles drained in a discrete event between two images. (b) Electrical conductivity (μS cm^{-1}). (c) suspended sediment concentration (kg m^{-3}; left-axis, black) and suspended sediment load (t d^{-1}; right-axis, red). (d) Temperature measurements from 450 m and 1480 m elevation. (e) 24-hour windowed correlation coefficient between Q and EC.

large spikes in SSC during P1, P2 and P4, and to a lesser extent, P3. These spikes precede the local discharge peaks and are characterized by a steep rise followed by a more gradual return to lower values. The SSC peak at P4 is the most dramatic and jumps from 2–>18 kg m^{-3} within 6 hours. The suspended sediment load (SSL) also grows throughout the season, and is significantly greater in the latter part of the season (Figure 2c). Prior to P4, SSL ranges from 0–4 × 10^4 t d^{-1}, and following P4 ranges from 4–20 × 10^4 t d^{-1}. The total suspended sediment flux for the survey period is ~4.7 ± 0.74 × 10^6 t.

4. Discussion

[10] The delay in the onset of significant runoff, following ~20 days with above-zero temperatures, can be explained by refreezing of an initial fraction of the surface melt in cold snow until the firn becomes isothermal [*Pfeffer et al.*, 1991] and observed ponding of surface meltwater. Prior to P1, low runoff volume and high EC indicate that water in the proglacial stream was derived substantially from leakage of basal meltwater from an inefficient winter drainage system beneath Leverett Glacier [*Collins*, 1979; *Skidmore and Sharp*, 1999].

[11] Using a temperature-index model [*Hock*, 2003] of surface melt within the catchment, calibrated with *in situ* measurements of initial snow depth and ablation, we found that the seasonal discharge volumes we observe cannot be explained by an increase in melt intensity within a stable catchment area (auxiliary material). Instead, the discharge observed at Leverett glacier can only be accounted for by progressive upglacier expansion of the catchment to include runoff from higher elevations through the melt season, indicating delivery of surface-generated meltwater from a progressively larger area of the ice sheet as the melt season develops. The required development and expansion of the contributing hydrological catchment, up to 800 melevation by June 6th, and to 1000 m by July 9th, eventually delivers surface meltwater from an area of over 600 km^2 that extends higher than 1200 m elevation and to a distance of >50 km from the ice margin by July 21st. The dramatic rise in runoff observed in the first half of July is driven, therefore, by a combination of high temperatures (Figure 2d) and recent expansion of the area of the ice sheet which delivers water to the ice margin via Leverett Glacier.

[12] The EC of meltwater can be used crudely to differentiate runoff components and hydrological pathways through a glacial catchment [*Collins*, 1979]. The basic pattern of decline from high to low solute concentration that we observe is typical of Alpine and High Arctic glaciers [*Collins*, 1979; *Skidmore and Sharp*, 1999] as the drainage system becomes more efficient and a greater proportion of water is transported rapidly through the glacier, limiting the potential for solute acquisition. Therefore, along with the upglacier expansion of the catchment in response to surface melt inputs, our data suggest a concomitant increase in its hydraulic efficiency throughout the melt-season.

[13] High suspended sediment concentrations indicate that meltwater emerging from Leverett Glacier has been routed from the ice sheet surface, where it was generated, via the ice sheet bed. Rates of basal sediment evacuation are controlled by the hydraulic efficiency of the subglacial drainage system, but can be limited by the availability of source material [*Alley et al.*, 1997; *Swift et al.*, 2002]. A sustained increase in subglacial hydraulic efficiency, and ongoing expansion of the subglacial drainage system, is consistent with the continued increase in SSC, even while runoff diminishes following peak discharge on July 16th [*Alley et al.*, 1997]. In addition, SSC shows no sign of supply exhaustion, suggesting that expansion of the efficient basal hydraulic system provides continual access to an extensive reservoir of basal sediment [*Swift et al.*, 2002].

[14] Spatial expansion of efficient subglacial drainage at the expense of a hydraulically inefficient distributed system explains temporal instability in the correlation between EC and Q on the rising limb of the seasonal discharge hydrograph. Upglacier expansion of supraglacial melt extent results in the upglacier expansion of the efficient subglacial drainage system through the delivery of surface meltwater to the glacier bed [*Nienow et al.*, 1998]. These surface waters initially drain into a hydraulically inefficient drainage system causing channel sections to grow in a downglacier direction until they connect with existing channels further downstream. Reduction of mean water pressure in the channels, relative to the distributed drainage system, is probably responsible for drawing out stored basal waters. Temporal and spatial evolution of the efficiency of the drainage system

therefore complicates the relationship between surface melting and proglacial runoff, especially during the period of each year when the subglacial system is becoming established. The stable hysteresis pattern that develops with EC peaking on the rising limb of the diurnal flow hydrograph, and the constant inverse relationship between EC and Q (Figure 2e), demonstrate that the hydrological system has reached a more stable and uniform configuration by July 16th.

[15] Observations on the GrIS have shown that moulins essentially comprise vertical conduits which transport water from the ice sheet surface to its bed [*Das et al.*, 2008; *Catania and Neumann*, 2010]. While there may be some lateral transport of water via englacial channels, in order to explain the trends in Q, EC and SSC we argue that opening of moulins at progressively higher elevations allows surface generated meltwater to be delivered to the ice sheet bed further inland through the melt season. Growth of the efficient subglacial system therefore follows upglacier development of supraglacial drainage and proceeds in a stepwise fashion as new input points become active 1998. This proposed model is analogous to one previously proposed for Alpine glacier drainage systems [*Nienow et al.*, 1998]. It is notable, therefore, that the channelized subglacial drainage system is sustained in the GrIS where ice thicknesses are much greater, implying that the high volumes of meltwater delivered to the glacier bed are sufficient to offset the increased potential for channel closure by deformation of thicker ice.

[16] Large rises in EC associated with P1, P2 and P4 suggest that a significant component of these flood-waters has a subglacial provenance and indicates the displacement of solute-rich stored water from an inefficient drainage system [*Skidmore and Sharp*, 1999]. Large sediment flushes (Figure 2c) also confirm interaction of meltwaters with the basal environment. They indicate sudden access of water to areas of subglacially stored sediments and a dramatic increase in the capacity of subglacial waters to mobilise and evacuate them [*Swift et al.*, 2002]. Rapid return to low EC values following each of the meltwater pulses implies that the hydraulic system downglacier already has the capacity to transport water quickly and efficiently.

[17] We suggest that P1, when the rise in EC is less dramatic than during P2 and P4, is the result of initial access of meltwater to the subglacial drainage system through moulins and crevasses low down on the glacier following the onset of spring melting. This is supported by observations of meltwater ponded in crevasses and supraglacial channels prior to P1, the drainage of which causes mixing with subglacially stored water and flushing of sediments from the winter drainage system as new channel sections develop. P3 is not accompanied by a dramatic rise in EC and therefore appears to be driven by changes in temperature-driven runoff feeding into the existing drainage system.

[18] P2 and P4 are superimposed on the rising limb of the seasonal hydrograph (Figure 2a) and cannot be explained by trends in surface melting (Figure 2d) as they occur during periods of low or zero ablation within the catchment. From the MODIS satellite images, we find that the timing of supraglacial lake drainage events, the size and elevation of the lakes (Figure 2a), and their location within the proposed catchment of Leverett Glacier (Figure 1), suggest that they are likely candidates for the source of the pulses of water during P2 and P4. In particular, P2 is associated with the drainage of five lakes between 800–1000 m, and P4 coincides with seven drainage events from lakes located between 1100–1200 m.

[19] Previous studies have found that MODIS classification of GrIS supraglacial lakes is robust when compared with higher resolution satellite data [*Sundal et al.*, 2009] and has an approximate error of 0.22 km^2. Estimation of lake area (Figure 2a), based on manual pixel counting of classified images [*Sundal et al.*, 2009], indicates that the lakes that drain at P2 have areas between 0.13 and 0.49 km^2 and those that drain at P4 are between 0.25 and 0.88 km^2. Using an average lake depth of 2.7 m (a value determined [*McMillan et al.*, 2007; *Shepherd et al.*, 2009] for ~150 lakes in this region in summer 2001), we find that the volume of water in each pulse (4.9 and 7.2 $\times$ 10^6 m^3 respectively) can be accounted for by the drainage of multiple lakes in a single event. Since there is uncertainty about the depth of individual lakes we are unable to determine which, or how many, of the lakes could contribute to each meltwater pulse. It is clear, however, that coincident with the observed pulses of meltwater (P2 and P4) a commensurate volume of meltwater drains from a number of lakes on the surface of the ice sheet within the catchment of Leverett glacier.

[20] We have observed active moulins at elevations of at least 1100 m in this region and supraglacial lakes that have drained through large crevasses in their centre at elevations up to 1450 m. A key role of these features in GrIS hydrology appears to be their contribution to the expansion of the subglacial area that is subject to inputs of surface meltwater and seasonal reorganization. Supraglacial lake drainage at high elevations may be particularly important for two reasons. Firstly it provides a mechanism for water to penetrate through thick, cold ice [*van der Veen*, 2007]. Secondly, concentration of surface meltwater into lakes may be critical to provide the volumes of water required to force evolution of a channelized drainage system beneath thick ice where overburden pressures are large.

[21] Our findings of seasonal upglacier-directed seasonal expansion of evolution in the subglacial drainage system and its conversion from a distributed to channelized system are supported by observations of ice-motion [*Bartholomew et al.*, 2010] and upglacier evolution in the timing of lake drainage [*Sundal et al.*, 2009] in this section of the ice sheet. Given recent focus within the glaciological community on the impact of channelized subglacial drainage on ice motion [*Schoof*, 2010; *Sundal et al.*, 2011] our findings provide a conceptual model of subaerial and supraglacial forcing of subglacial drainage development which can be incorporated in numerical experiments designed to investigate the relationship between surface melting and ice velocity in the GrIS [*Schoof*, 2010; *Pimentel and Flowers*, 2011].

5. Conclusions

[22] Our observations provide the first synopsis of the seasonal hydrological behaviour of a large (>600 km^2) catchment in the ablation zone of the GrIS, showing how surface meltwater production drives spatial and temporal changes in the subglacial drainage system. These observations show the development and expansion of a drainage system that delivers water from the ice surface, via the ice-sheet bed, to the margin. This system expands progressively throughout the ablation season to >50 km from the ice

margin. We propose a model that is similar to one proposed for Alpine systems, where the drainage system becomes increasingly efficient as hydraulic connections between the surface and bed are established further inland, evacuating large volumes of meltwater and sediment.

[23] **Acknowledgments.** We thank for financial support: UK Natural Environment Research Council (NERC, through a studentship to IB and grants to PN/DM), Edinburgh University Moss Centenary Scholarship (IB). ERS SAR data, for the surface DEM, were provided by the European Space Agency VECTRA project (SP).

[24] The Editor thanks Martin Sharp and an anonymous reviewer for their assistance in evaluating this paper.

References

Alley, R., K. Cuffey, E. Evenson, J. Strasser, D. Lawson, and G. Larson (1997), How glaciers entrain and transport basal sediment: Physical constraints, *Quat. Sci. Rev.*, *16*(9), 1017–1038.

Bartholomew, I., P. Nienow, D. Mair, A. Hubbard, M. King, and A. Sole (2010), Seasonal evolution of subglacial drainage and acceleration in a Greenland outlet glacier, *Nat. Geosci.*, *3*, 408–411.

Box, J., and K. Ski (2007), Remote sounding of Greenland supraglacial melt lakes: Implications for subglacial hydraulics, *J. Glaciol.*, *53*(181), 257–265.

Catania, G. A., and T. A. Neumann (2010), Persistent englacial drainage features in the Greenland ice sheet, *Geophys. Res. Lett.*, *37*, L02501, doi:10.1029/2009GL041108.

Collins, D. (1979), Hydrochemistry of meltwaters draining from an alpine glacier, *Arct. Alp. Res.*, *11*(3), 307–324.

Das, S., I. Joughin, M. Behn, I. Howat, M. King, D. Lizarralde, and M. Bhatia (2008), Fracture propagation to the base of the Greenland ice sheet during supraglacial lake drainage, *Science*, *320*(5877), 778.

Fenn, C. (1987), Electrical conductivity, in *Glacio-fluvial Sediment Transfer: An Alpine Perspective*, edited by A. M. Gurnell and M. J. Clark, pp. 377–414, John Wiley, Chichester, U. K.

Hock, R. (2003), Temperature index melt modelling in mountain areas, *J. Hydrol.*, *282*(1–4), 104–115.

Kamb, B. (1987), Glacier surge mechanism based on linked cavity configuration of the basal water conduit system, *J. Geophys. Res.*, *92*(B9), 9083–9100

McMillan, M., P. Nienow, A. Shepherd, T. Benham, and A. Sole (2007), Seasonal evolution of supra-glacial lakes on the Greenland Ice Sheet, *Earth Planet. Sci. Lett.*, *262*, 484–492.

Nienow, P., M. Sharp, and I. Willis (1998), Seasonal changes in the morphology of the subglacial drainage system, Haut Glacier d'Arolla, Switzerland, *Earth Surf. Processes Landforms*, *23*(9), 825–843.

Palmer, S., A. Shepherd, P. Nienow, and I. Joughin (2011), Seasonal speedup of the Greenland ice sheet linked to routing of surface water, *Earth Planet. Sci. Lett.*, *302*, 423–428.

Parizek, B., and R. Alley (2004), Implications of increased Greenland surface melt under global-warming scenarios: Ice-sheet simulations, *Quat. Sci. Rev.*, *23*(9–10), 1013–1027.

Pfeffer, W. T., M. F. Meier, and T. H. Illangasekare (1991), Retention of Greenland runoff by refreezing: Implications for projected future sea level change, *J. Geophys. Res.*, *96*(C12), 22,117–22,124.

Pimentel, S., and G. Flowers (2011), A numerical study of hydrologically driven glacier dynamics and subglacial flooding, *Proc. R. Soc. A*, doi:10.1098/rspa.2010.0211, in press.

Schoof, C. (2010), Ice-sheet acceleration driven by melt supply variability, *Nature*, *468*(7325), 803–806.

Shepherd, A., A. Hubbard, P. Nienow, M. King, M. McMillan, and I. Joughin (2009), Greenland ice sheet motion coupled with daily melting in late summer, *Geophys. Res. Lett.*, *36*, L01501, doi:10.1029/2008GL035758.

Shreve, R. (1972), Movement of water in glaciers, *J. Glaciol.*, *11*(62), 205–214.

Skidmore, M., and M. Sharp (1999), Drainage system behaviour of a high-Arctic polythermal glacier, *Ann. Glaciol.*, *28*(1), 209–215.

Sundal, A., A. Shepherd, P. Nienow, E. Hanna, S. Palmer, and P. Huybrechts (2009), Evolution of supra-glacial lakes across the Greenland ice sheet, *Remote Sens. Environ.*, *113*, 2164–2171.

Sundal, A., A. Shepherd, P. Nienow, E. Hanna, S. Palmer, and P. Huybrechts (2011), Melt-induced speed-up of Greenland ice sheet offset by efficient subglacial drainage, *Nature*, *469*(7331), 521–524.

Swift, D., P. Nienow, N. Spedding, and T. Hoey (2002), Geomorphic implications of subglacial drainage configuration: rates of basal sediment evacuation controlled by seasonal drainage system evolution, *Sediment. Geol.*, *149*(1–3), 5–19.

Van de Wal, R., W. Boot, M. Van den Broeke, C. Smeets, C. Reijmer, J. Donker, and J. Oerlemans (2008), Large and rapid melt-induced velocity changes in the ablation zone of the Greenland ice sheet, *Science*, *321*(5885), 111.

van der Veen, C. J. (2007), Fracture propagation as means of rapidly transferring surface meltwater to the base of glaciers, *Geophys. Res. Lett.*, *34*, L01501, doi:10.1029/2006GL028385.

Zwally, H., W. Abdalati, T. Herring, K. Larson, J. Saba, and K. Steffen (2002), Surface melt-induced acceleration of Greenland ice-sheet flow, *Science*, *297*(5579), 218.

I. Bartholomew, T. Cowton, P. Nienow, and A. Sole, School of Geosciences, University of Edinburgh, Drummond Street, Edinburgh EH8 9XP, UK. (ian.bartholomew@ed.ac.uk; t.r.cowton@sms.ed.ac.uk; peter.nienow@ed.ac.uk; andrew.sole@ed.ac.uk)

D. Mair, School of Geosciences, University of Aberdeen, Elphinstone Road, Aberdeen AB24 3UF, UK. (d.mair@abdn.ac.uk)

S. Palmer, School of Earth and Environment, University of Leeds, Maths/Earth and Environment Building, Leeds LS2 9JT, UK. (s.j.palmer@leeds.ac.uk)

J. Wadham, School of Geographical Sciences, University of Bristol, University Road, Bristol BS8 1SS, UK. (j.l.wadham@bristol.ac.uk)